DR. DAIJIANG LI (Orcid ID : 0000-0002-0925-3421)

Article type : Primary Research Articles

Climate, urbanization, and species traits interactively drive flowering duration

Daijiang Li[1,2,3†], Narayani Barve[1], Laura Brenskelle[1], Kamala Earl[1], Vijay Barve[1], Michael W. Belitz[1], Joshua Doby[1], Maggie M. Hantak[1], Jessica A. Oswald[1,4], Brian J. Stucky[1], Mitch Walters[1], Robert P. Guralnick[1†]

21 November, 2020

[1] Florida Museum of Natural History, University of Florida, Gainesville, FL, USA
[2] Department of Biological Sciences, Louisiana State University, Baton Rouge, LA, USA
[3] Center for Computation & Technology, Louisiana State University, Baton Rouge, LA, USA
[4] Biology Department, University of Nevada Reno, Reno, NV, 89557, USA
[†] Corresponding authors: daijianglee@gmail.com; rguralnick@flmnh.ufl.edu

Running head: Flower duration along environmental gradients

Abstract: A wave of green leaves and multi-colored flowers advances from low to high latitudes each spring. However, little is known about how flowering offset (i.e., ending of flowering) and duration of populations of the same species vary along environmental gradients. Understanding these patterns is critical for predicting the effects of future climate and land-use change on plants, pollinators, and herbivores. Here, we investigated potential climatic and landscape drivers of flowering onset, offset, and duration of 52 plant species with varying key traits. We generated phenology estimates using >270,000 community-science photographs and a novel presence-only phenometric estimation method. We found longer flowering durations in warmer areas, which is more obvious for summer-blooming species compared to spring-bloomers driven by their strongly differing offset dynamics. We also found that higher human population density and higher annual precipitation are associated with delayed flowering offset and extended flowering duration. Finally, offset of woody perennials was more sensitive than herbaceous species to both climate and urbanization drivers. Empirical forecast models suggested that flowering durations will be longer in 2030 and 2050 under representative concentration pathway (RCP) 8.5, especially for summer-blooming species. Our study provides critical insight into drivers of key flowering phenophases and confirms that Hopkins' Bioclimatic Law also applies to flowering durations for summer-blooming species and herbaceous spring-blooming species.

Key words: Plant phenology, Urbanization, Climate change, Flower duration, Hopkins' Bioclimatic Law

1 Introduction

It is well known that leaf out and flowering onset occur earlier at lower latitudes and altitudes, a pattern referred to as Hopkins' Bioclimatic Law (Hopkins 1920). The production of leaves and flowers provides critical resources and cues to other members of the community, such as insects, with consequences for ecosystem productivity and carbon uptake (Visser and Both 2005, Cleland et al. 2007, Parmesan 2007). However, it is far less known whether the senescence of leaves and offset (i.e., ending) of flowering are also sensitive to environmental conditions to the same extent as onset. Consequently, it is unclear whether the duration of such reproductive events changes over these same latitudinal and elevational gradients. Do populations of the same plant species have longer flowering seasons in warm areas compared to those in cold areas? Or is the duration of flowering constant across regions? How will future environmental changes affect shifts in onset, offset, and length of flowering? These answers have significant implications for ecosystem functioning, for example via mismatches with pollinators (Kudo and Ida 2013, Schenk et al. 2018), thereby directly impacting plant fitness and ecosystem health (Petanidou et al. 2014, Rafferty et al. 2016).

The timing of flowering onset is known to be tuned to environmental conditions that are rapidly changing, including temperature and precipitation during growing seasons, and winter chilling

(Mouradov et al. 2002, Larcher 2003, Cleland et al. 2007, Zohner et al. 2018). Extensive continuing development of human-built environments contributes to and interacts with climate, while also increasing air pollution and altering soils and hydrology (Grimm et al. 2008). These accelerating landscape changes also impact plant flowering phenology in complex ways (Jochner and Menzel 2015). Li et al. (2019), for example, demonstrated that the impact of urbanization on flowering and leaf-out timing depends on the context of the regional temperature and is not simply driven by urban heat island effects. These interactions between global-scale patterns such as climate warming, and more regional landscape changes, make clear the importance of modeling frameworks that are able to incorporate multiple drivers operating at different spatial scales, and how they intersect with species life-history traits, to better understand spatial and temporal patterns of flowering phenology change.

Previous studies have implicated both genetic control and environmental cues as drivers of offset and duration. Recent work in the Arctic has shown that while onset may be controlled by environmental factors such as snowmelt, offset does not have direct environmental cueing and is likely under genetic control (Semenchuk et al. 2016). In such cases, flowering duration would not be impacted by climate change. Shifting onset but fixed durations could exacerbate phenological mismatch, especially if pollinator activities do not also shift in the same way (Kudo and Ida 2013, Renner and Zohner 2018). Other work has shown that flowering offset has complex cueing that often includes temperature driving earlier offset (Høye et al. 2013, Marchin et al. 2015). If different cues drive onset and offset, increased warming could lead to longer or shorter durations (Fig. 1), rather than simply shifting flowering timing. It remains poorly understood whether there are generalities to onset, offset, and duration of flowering, and whether these events are mediated by key environmental cues or underlying phylogenetic constraints.

Previously, the major challenge with assessing environmental drivers of phenophases beyond onset was a lack of data to examine trends over space or time. Community-science photographs of plants are a key resource that hold promise for providing the data needed for such analyses (Barve et al. 2020), but have so far been underused. Such resources have grown exponentially in recent years. As of June 2020, the community-science platform iNaturalist has over 5 million research-grade photographs of over 16,000 angiosperm species in the United States alone, and total records are doubling in growth per year. Openly available iNaturalist record data provide a unique opportunity to study phenology trends at broad extents and finer spatial resolutions than ever before.

Here we use a novel suite of methods and data resources to understand how flowering onset, offset, and duration vary across space and in relation to both climate and urbanization. In particular, we focus on 52 species of common flowering plants that differ in their flowering onset timing and in functional aspects of growth form and reproduction - traits that are expected to relate to differential response to climatic conditions (Sherry et al. 2007, Wang et al. 2020). Understanding how traits condition the phenological responses of species is critical to predicting the impacts of anthropogenic change. We also predict likely responses to future warming and urbanization, and discuss challenges inherent in predictions based on such space-for-time substitutions. In particular, we address three key questions: 1) How is the timing and duration of flowering affected by climate and how do species traits mediate those effects? 2) How does urbanization influence the timing and duration of flowering? 3) How will the timing and duration of flowering change over the next 30 years with ongoing land-use and climate change?

2 Methods

2.1 Phenological Data

We downloaded all images for the records marked as research grade for 60 flowering plant species from iNaturalist (accessed between 7th February 2020 to 31st March 2020). Research-grade photographs are those for which at least two iNaturalist users have verified identifications and are considered usable in downstream research activities. We chose an initial list of 60 species strategically based on the following criteria: 1) Species must have broad distributions across latitude in order to capture variation across climate gradients. 2) Species must have flowers that are easy to visually score as present or absent. We prioritized plants with large, showy flowers. 3) Species must also have sufficient numbers of research-grade observations. We required a minimum of 1,000 research grade observations for initial consideration, but as discussed below, the actual number of records with flowers that were found in a sufficient number of spatial grids was unknown until later in the pipeline. 4) Species were chosen to balance sampling of key traits used in the analysis. These selected focal traits included whether the plant was annual or perennial, woody or herbaceous, and whether the plant was an early spring, late spring, or summer blooming species. Trait data were gathered from literature sources or online resources and are available in Supporting Data 1.

After downloading images, we used the software ImageAnt (https://gitlab.com/stuckyb/imageant) to score the presence of flowers in photographs. We set up a scoring rubric in ImageAnt that had four states, “present”, “absent”, “uncertain” or “flag due to a problem”. We considered a photograph to have flowers absent if no flowers were visible on the photograph, or if all the inflorescences on a sheet had wilted, dried or discolored petals or other structures. If a photograph had multiple senesced flowers but a single one that was not wilted, dried or discolored, these were scored as evidence of flower presence. We used a presence-only modeling approach for estimating onset and offset because the absence of a flower in a photograph does not guarantee true absence unless the whole plant is photographed, which is often not the case. As well, presence-only based predictions of onset and offset have been recently shown to be robust when using proper methods, based on simulation results (Belitz et al. 2020). We used scoring of “uncertain” in cases where a definitive flowering state could not be determined. We found a very small percent (less than 0.1%) of the images for which taxonomic misidentification or image problems, which we flagged.

We tested how well flowers could be reliably annotated by scorers by initially requiring each image be scored by at least two independent volunteers for 10 test species, following the protocol proposed by Barve et al. (2020). Scores were compared between volunteers, and given a low rate of disagreement (< 1%), we opted for a simpler single-annotator approach. In total, 270,111 images were scored for 52 species. We then filtered records that were scored as presence, removing absence, uncertain and flagged records, resulting in 205,993 records with flowers present. We further focused on the 160,097 records that were observed between 2017 and 2019 because our goal is to study spatial patterns (See Supporting Data 1 for per-species details).

2.2 Estimate flowering onset, offset, and duration

We divided the contiguous United States into 25 km by 25 km grid cells using the Albers Equal Area projection (Fig. 1) and estimated the flowering onset, offset, and durations for species-year-grid cell combinations with enough records (see below for details). These data represent an aggregated population-level estimate of onset and offset in order to examine broad climate and landscape gradients. In several species-year-grid cell combinations, some particular days, within iNaturalist's City Nature Challenge window, had significantly more images than others, which may bias the estimations of flowering onset and offset. We reduced potential biases by randomly thinning the images from those dates to the average number of images per day for that species-year-grid cell combination. For each species-year combination, we only included grid cells with at least 10 scores from at least 3 different dates, resulting in 54,559 records from 52 species and 484 unique grid cells. For each of the 2,281 species-year-grid cell combinations, we estimated flowering onset and offset based on the image dates using a newly developed R package, `phenesse` v0.1.1 (Belitz et al. 2020). Phenesse uses a parametric bootstrapping approach to estimate phenological metrics for any percentile using the Weibull distribution and has been demonstrated to provide accurate and unbiased estimates for unimodal seasonal abundance curves (Belitz et al. 2020). We used the estimates of 5 and 95 percentiles as proxies for flowering onset and offset, as these phenometrics have been found to be more accurate and less biased than attempting to estimate the absolute start and termination of a flowering event (Belitz et al. 2020). Durations were calculated as the number of days between the estimated flowering onset and offset dates. In very few species-year-grid cell combinations (< 10), the flowering duration was estimated to be more than 365 days. We floored those cases to 365 days, representing year-round flowering.

2.3 Contemporary and future Environmental Data

For each species-year-grid cell combination with estimates of flowering onset, offset, and duration, we obtained two types of environmental variables: climate and human population density (`pop`, as a proxy for urbanization). For climatic variables, we extracted annual average temperature (`bio1`), temperature seasonality (`bio4`), annual precipitation (`bio12`), and precipitation seasonality (`bio15`) for the corresponding year (2017, 2018, or 2019) based on monthly data from PRISM (PRISM Climate Group 2004). These variables provide broad climatic background and are known to affect plant flowering phenology. Besides the broad climatic background, plants are affected by winter chilling. We counted a day as a chilling day if its daily average temperature was between 0 and 7.2 °C. We calculated the number of chilling days from November 15 to the end of February for all species-year-grid cell combinations based on daily climate data from PRISM (PRISM Climate Group 2004). We estimated human population density value for each grid cell and used it as a proxy for urbanization (cf. Li et al. 2019). We used the 2010s human population density data from Fang and Jawitz (2018), who provided decadal human population density data for the USA since 1790 at 1 km by 1 km spatial resolution.

For each grid cell, we also made predictions based on future climate and population density projections. We estimated projected human population density at 2030 and 2050 using data provided by McKee et al (2015). For future climate data, we used the NASA NEX-DCP30 dataset (Thrasher et al. 2013) and the NASA NEX-GDDP dataset (Thrasher et al. 2012). Both datasets were derived from the General Circulation Model (GCM) runs conducted under the Coupled Model Intercomparison Project Phase 5 (CMIP5) (Taylor et al. 2012) and across different greenhouse gas emission scenarios known as Representative Concentration Pathways (RCPs) (Meinshausen et al. 2011). Both datasets included ensemble statistics calculated for each RCP from all model runs available (33 models and 21 models, respectively). The NASA NEX-DCP30 dataset provides downscaled monthly projections of temperature and precipitation from 2006 to 2099 while the NASA NEX-GDDP dataset provides daily projections. Raster files for all environmental variables were first reprojected and aggregated to have the same spatial extent and resolution as the flowering phenological data before extracting contemporary and future values.

From the NASA NEX-DCP30 datasets, we calculated bio1, bio4, bio12, and bio15 for each grid cell from 2025 to 2034 and from 2045 to 2054 based on the NASA NEX-DCP30 monthly data. We used the average value from 2025 to 2034 as the value of bioclimatic variables of 2030 and the average value from 2045 to 2054 as the value of bioclimatic variables of 2050. We calculated the number of chilling days during winter for the year 2030 and 2050 based on the NASA-GDDP dataset. Given the large data files and the computational burden, we did not use 10-year averages for the number of chilling days. For all projected climate data, we chose the RCP 8.5 emissions scenario because the current emissions trajectories have more closely followed RCP 8.5 than the lower RCP scenarios (Peters et al. 2012).

2.4 Plant traits and phylogeny

We collected trait information for 52 plant species from relevant literature and websites (Fig. S1). Previously reported flowering durations were represented as a range of months. Based on reported flowering durations, we classified species onset into early spring (Feb-March), late spring (April-May), or summer(June-Sep). Exploratory data analysis suggested no differences between early and late spring species, so we lumped both groups as spring bloomers, defined as plants whose flowering onset is earlier than June. We also grouped species into one of the following three broadly defined growth forms: Herb_annual/biennial, Herb_perennial, and Woody_perennial. We derived a phylogeny (Fig. S1) for our 52 focal species from Smith and Brown (Smith and Brown 2018), who provided one of the most comprehensive seed plant phylogenies with branch lengths, based on the Open Tree of Life (Hinchliff et al. 2015).

2.5 Statistical Analysis

To study how environmental variables, including urbanization, affect flowering onset, offset, and duration and whether such effects vary with species' traits, we used linear mixed models (LMM). We used the same process to select predictors and build models for flowering onset, offset, and duration. We started with all of the environmental variables as predictors (bio1, bio4, bio12, number of chilling days in winter, and population density) and phenology (either onset day of year, offset day of year, or number of days for duration) as the response variable. Additionally, we added important two-way interactions in the model. Models included the identity of grid cells and species as random terms for intercept, and species as random term for slope for each of the environmental variables. We did not include bio15 in all analyses because it is highly correlated with bio4 and bio12 (Fig. S2). We also examined growing degree day (GDD) models, considering GDDs accumulated in the 90 days prior to onset or offset predictions, but these were consistently highly correlated with mean annual temperature ($r > 0.9$) and cannot be used for duration predictions. Instead of adding all possible combinations of interactions, we only included two-way interaction terms that make biological and ecological sense based on our understanding of plant physiology and phenology in the model. Specifically, we added `bio1:pop.`, `bio12:pop`, and `bio1:bio12` in all starting models based on previous literature (Jochner and Menzel 2015, Li et al. 2019).The first two interaction terms test whether the effects of human population density (i.e., urbanization) on plant flowering vary across regions with different climatic conditions. The third interaction term tests whether the effect of average temperature changes along a precipitation gradient. We separately ran models with number of records in a grid cell as covariate, in order to test if sampling biases impacted results, and in all cases found that this predictor was not explanatory.

We then used the `step()` function from the R package `lmerTest` v3.1-2 (Kuznetsova et al. 2017) to conduct backward model selections. After the best environmental variable model was found, we added the two plant traits: blooming groups (Spring or Summer) and growth forms (Herb_annual/biennial, Herb_perennial, and Woody_perennial) into the model, along with their two-way interactions with each environmental variable. Such trait-environment interaction terms tested whether the changes of plant flowering phenology along environmental gradients differ among plant species with differing traits. We conducted backward model selections again to get the final models for flowering onset, offset, and duration.

All environmental variables were scaled to have mean 0 and standard deviation 1 before model fittings so that their effect sizes are comparable. Exploratory data analyses did not show any obvious differences across different years for each species-grid cell combination. We thus ignored the year in all models. Final models were fitted using R package `lme4` v1.1-23 (Bates et al. 2015) with P-values calculated with the R package `lmerTest` v3.1-2 (Kuznetsova et al. 2017). We checked residuals of all three final models and did not find obvious deviation from model assumptions, including spatial autocorrelations (Fig. S3). Ignoring the phylogenetic relationships among species when fitting Linear Mixed Models with multiple species like ours may lead to badly inflated type I errors (false positives) (Li and Ives 2017). Therefore, we checked the three final models with phylogenetic linear mixed models that account for phylogenetic relationships among species using the R package `phyr` v1.0.2 (Li et al. 2020). We used the Bayesian framework to re-fit the final models with uninformative priors, as it handles data with large numbers of levels in random terms better than the maximum likelihood framework in `phyr`. The results were largely the same (Table S5 – S7), confirming the results based on Linear Mixed Models. We thus reported results based on LMMs in the main text.

To predict plant flowering onset, offset, and duration of each species-grid cell combination in 2030 and 2050, we used predicted annual mean temperature, annual temperature seasonality, annual precipitation, number of chilling days in winter, and forecast human population density in 2030 and

2050 with the assumption that the plant species observed in each grid cell will still occur there in those years. Given that the traits we used are categorical and describe the life-history of plants, they should not change by 2050. We used the `predict()` function in the R package `lme4` keeping all random effects. For each species-grid cell combination, we then calculated the differences between the forecast flowering onset, offset, and duration with those observed (`Δonset`, `Δoffset`, `Δduration`). For `Δonset` and `Δoffset`, positive values represent flowering delays while negative values represent advances; positive `Δduration` values represent longer flowering duration while negative values represent shorter duration. To statistically describe the changes in plant flowering phenology, we fitted simple Linear Mixed Models for `Δonset`, `Δoffset`, and `Δduration` with intercept as the only fixed term and species as the only random term for the intercept. Such simple models allowed us to look at the general trends across all species as well as species-specific changes over time.

3 Results

Flowering Onset. The best flowering onset model included temperature, temperature seasonality, and number of winter chilling days. Human population density and precipitation variables were not included in top models nor was plant growth form. This model also included a strong interaction effect between annual temperature and flowering onset. All of the model predictors were highly significant ($p < 0.005$, Fig. 2, Table 1, Table S1). Annual temperature was the strongest climate predictor for spring onset, but its effect depends on timing of onset (spring versus summer). Holding other variables constant, a 1 standard deviation (s.d.) increase of temperature (about 3.94 °C) advanced flowering onset of species blooming in spring about 16.2 ± 1.6 days (uncertainty is reported as standard error hereafter) but only advanced ~6 ± 2.7 days for summer bloomers (Fig. 2a). For temperature seasonality, a 1 s.d. increase delayed flowering onset about 7.8 ± 1.7 days (Fig. 2b) and a 1 s.d. increase of the number of chilling days in winter (about 20 days) delayed flowering onset about 3.3 ± 1 days (Fig. 2c).

Flowering Offset. Key predictors of flowering offset included temperature, human population density, and especially onset timing (Fig. 3, Table 1, Table S2). As in the onset models, there was a strong interaction between onset timing and annual temperature. Unlike the onset models, there were strong growth-form interactions with population density and precipitation. The average day of year of flowering offset for herbaceous annual spring bloomers was around 146 ± 11.9 (end of May), while herbaceous annual summer bloomers typically have flowering offset around 128 ± 12.4 days later than those of spring bloomers (end of September, $p < 0.001$, Table S2). The effects of average annual temperature on flowering offset differ between blooming groups (χ_1^2 = 111.91, $p < 0.001$). Holding other variables constant, a 1 s.d. increase in annual average temperature (about 3.94 °C) advanced flowering offset of spring bloomers about 16.7 ± 1.5 days, but delayed flowering offset for summer bloomers about 8.7 ± 2.4 days (Fig. 3a). The effect of human population density on flowering offset varied among different growth forms (χ_2^2 = 22.04, $p < 0.001$), with woody perennial species being affected the most (Fig. 3b). A 1 s.d. increase of log10-transformed human population density, that is about 0.8 order of magnitude change, delayed flowering offset of woody perennials about 12.2 ± 2.3 days (Fig. 3b), which is a much stronger effect than for herbaceous plants. Woody perennial species were also affected the most by annual precipitation: a 1 s.d. increase of annual precipitation (about 437 mm) delayed their flowering offset about 6.1 ± 2.8 days (Fig. 3c).

Flowering Duration. Flowering duration models had a complex set of predictors (Fig. 4, Table 1, Table S3). The average flowering duration for plants with flowering onset in spring versus summer was around 53.8 ± 4.2 and 93.8 ± 6.6 days, respectively (Fig. 4e). Woody perennials had longer flowering duration (93.9 ± 10.8 days) than herbaceous annual/biennials (71.3 ± 6.9 days) and herbaceous perennials (57.3 ± 4.5 days) (χ_2^2 = 14.06, $p < 0.001$, Fig. 4f). Effects of annual average temperature (bio1) on flowering duration varied between species that have flowering onset in spring versus summer (χ_1^2 = 15.06, $p < 0.001$) and across growth forms (χ_2^2 = 11.14, $p = 0.004$, Fig. 4a). For herbaceous annuals, a 1 s.d. increase of annual average temperature (about 3.94 °C) extended flowering duration of spring bloomers by about 9.3 ± 3 days but extended flowering duration for summer bloomers by about 19.7 ± 2.7 days (Table 1, Table S3). The trend that flowering duration of plants with summer onset extended faster with increasing temperature than those with spring onset holds for all growth forms (Fig. 4a). Increasing human population density extended flowering duration of summer-blooming species, but not spring bloomers (Fig. 4b). A 1 s.d. increase of log10-transformed human population density (about 0.8 order of magnitude) extended flowering duration of summer bloomers by about 4.1 ± 2 days (Table 1, Table S3). Flowering durations of woody perennials were more sensitive to temperature seasonality than herbaceous perennials and herbaceous annual/binniels (Fig. 4c). Despite the significant effect of precipitation on flowering offset, its effect on flowering duration was not significant (slope = 1.62, p = 0.157, Fig. 4d). Flowering duration decreased significantly with an increased number of chilling days in winter (slope = 6.05, p < 0.001, Fig. 4g).

Flowering Timing and Duration Predictions in 2030 and 2050. We used model results and spatially-explicit scenarios of climate change (Representative Concentration Pathways [RCP] 8.5) and human population density for the years 2030 and 2050 to forecast flowering onset, offset and duration. Under RCP 8.5, average flowering onset dates will advance (i.e., earlier in the year) by 4.84 ± 0.4 and 8.04 ± 0.6 days across all species in 2030 and 2050, respectively (Fig. 5). In both years, flowering onset dates for both spring and summer bloomers are predicted to advance, but species with spring onsets will advance more (Table S4). For both blooming groups, flowering onset dates are predicted to advance more in 2050 than in 2030. Average flowering offset dates will advance less than changes in flowering onset, with about 3.54 ± 0.5 and 5.65 ± 1 days across all species in 2030 and 2050, respectively (Fig. 5). Flowering offset dates of spring bloomers are predicted to advance in both 2030 and 2050, with larger advances in 2050 (Table 5). However, flowering offset dates of summer bloomers are predicted to delay in 2030 and even further in 2050. Average flowering durations across all species will be about 2.99 ± 0.7 and 3.74 ± 0.9 days longer in 2030 and 2050, respectively (Fig. 5). In both years, predicted increases in flowering duration of summer bloomers were significantly larger than those in spring-blooming species (Table S4). Furthermore, the predicted increases in flowering duration of spring bloomers did not change from 2030 to 2050 while those of summer bloomers are predicted to become larger (Table S4).

4 Discussion

Changes in the timing and duration of flowering may disrupt interactions between plants and their pollinators, herbivores, and pathogens, reducing fitness at multiple trophic levels (Kudo and Cooper 2019). Here, for the first time, we have collected macroscale, multi-species data to understand how flowering timing and duration varies across broad environmental gradients. This approach has its roots in the pioneering work of Andrew Delmar Hopkins and his Bioclimatic Law (Hopkins 1920), which postulated generalities about the timing of phenological events across climatic gradients. Our work, nearly a century later, uses new data resources and methods to highlight the importance of interactions between climate, urbanization, and species traits for conditioning offset and duration of flowering. These models provide a needed basis for first-of-its-kind forecasting of flowering timing and durations under climate change and urbanization.

Our work provides a starting basis for understanding shifts in both flowering onset and offset and the overall effect on flowering duration. The few previous studies that focused on flowering duration have been limited to local spatial extents. Lessard et al. (2014) is notable for taking a phylogenetic comparative approach to examining flowering duration, focusing on communities along elevational gradients in the Canadian subarctic. They found that flowering durations were fixed while onset dates advanced. In warmer areas such as temperate and subtropical regions, most studies have instead found varying flowering durations across spatial gradients, over time, or via experimental warming treatments (Sherry et al. 2007, Rafferty et al. 2016, Stinson et al. 2016) but generalities have yet to emerge. Here we find that flowering duration generally increases in areas that are warmer and less seasonal. However, these effects are strongly conditioned by species traits, such that full understanding of changes in duration of flowering must take these traits into account. In particular, we found a strong interaction between temperature and general timing of flowering onset. Plants that flower in summer have much longer durations in the warmer parts of their range than those in colder regions, compared to plants that flower in spring. As an example, holding everything else equal, an eight degree difference in annual mean temperature would lead to an average 20 day longer duration for spring-blooming species, but a 40 day longer duration for summer-blooming species. When including such trait and climate interactions in our multi-species mixed models, we found highly explanatory models for both offset and duration. These results were particularly unexpected given that Crimmins et al. (2013) found a very different result in a more arid community along an elevational gradient, where summer flowering species had generally shorter durations.

These significant differences in duration are strongly determined by onset and offset differences in spring and summer-blooming plants. Increasing annual temperatures drive earlier onset in both spring and summer-blooming plants, although its effects are stronger for spring-blooming plants. However, increasing annual temperature advances offset in spring-blooming plants, but instead delays offset for summer bloomers. This is because most summer plants are in bloom continuously until fall conditions, such as the first frost, cause flower senescence. Spring-flowering plants, by contrast, are more often ephemeral bloomers, especially herbaceous plants in forested areas that need to flower before canopies completely close and limit available light. This fundamental difference is key, and may better explain general patterns seen in the literature concerning advancing spring flowering onset and delayed autumn senescence (Menzel and Fabian 1999, Linderholm 2006). We note that we explicitly selected species from a range of habitats and ecoregions in order to better derive a general view of drivers of flowering offset and duration. However, we expect particular climate contexts may not conform, in particular arid environments (Crimmins et al. 2013). Yet broader sampling and explicit incorporation of habitat and ecoregion in models will likely provide an even stronger basis for predicting flowering phenology response to climatic change.

Previous work has also suggested the importance of growth form for explaining variation in phenological sensitivity to climate (Richardson and O'Keefe 2009, Wang et al. 2020). Larger shrubs and trees may be able to intercept more light compared with understory herbaceous plants, suggesting stronger direct effects compared to more climatically buffered understory plants. Our results align with these predictions, with increased sensitivity of woody plants compared to herbaceous ones, whether perennial or annual. We also note that results for all models are robust when accounting for phylogenetic autocorrelation (Table S5 – S7), as ignoring phylogenetic relationships may inflate type I errors of regressions (Felsenstein 1985, Garamszegi 2014, Li and Ives 2017). Finally, we note that more winter chilling days surprisingly led to later flowering onset, which is opposite predictions that fewer chilling days delays onset (Murray et al. 1989). Inclusion of species without chilling requirements, local adaptation across spatial gradients for those species that do, and the relatively strong relationship between winter chilling and temperature seasonality (Fig. S2) may all contribute to this positive relationship.

Increasing human population density (i.e., urbanization) did not show a strong pattern with flowering onset, but did delay flowering offset, consequently extending flowering duration (especially for summer-blooming species). Li et al. (2019) found that urbanization interacts with temperature to drive flowering phenology, using data mostly from the USA-National Phenology Network (USA-NPN).

That study focused on median open flower timing, rather than onset or offset, limiting direct comparisons with this study. Further comparisons across datasets are challenging due to a paucity of flower senescence timing data at USA-NPN. Still, both Li et al. (2019) and our work confirm that urbanization is a driver of flowering phenology. Less clear is why flowering offset, but not onset, should be affected by urbanization, especially if the pattern is mostly driven by urban heat island effects (UHI). It may be that the UHI effects were not strong enough in spring to affect onset but were strong enough to affect offset. We note that urbanization effects were stronger for summer-blooming species, where UHI might provide a buffer against late-season cold snaps (Yang and Bou-Zeid 2018). It is also likely that urban heat islands are not the only impact of urban environments on plant phenology (Li et al. 2019, Wohlfahrt et al. 2019). More work is needed to compare flower offset and duration dynamics in urban versus non-urban settings.

These results have strong implications for how continued warming and human development will impact flowering duration, and the ecological processes to which it is linked. Our empirically derived forecast models suggest that warming climate and urbanization trends are likely to lead to longer flowering durations. Longer durations, especially for summer-blooming plants, may mitigate the effects of onset shifts in relation to phenological mismatch with insect pollinators, presuming pollinators are responding to different cues. Based on the interactions between plant traits and temperature revealed here, durations may lengthen, especially for summer-flowering plants in areas where warming and/or urbanization increase the most. For spring-blooming species, flowering duration will likely be longer by 2030 but will be shorter by 2050, when their flowering offset will be advanced more than their onset. Such trait-dependent shifts in flowering timing and duration will affect fitness and cause phenological reassembly of plant communities (CaraDonna et al. 2014, Theobald et al. 2017), which in turn can strongly influence biotic interactions (Wolkovich and Cleland 2011), leading to trophic mismatches and altering food webs and ecosystem functioning (Tylianakis et al. 2008, Kerby and Post 2013, Visser and Gienapp 2019).

Estimating the absolute bounds of phenological events can be highly biased and inaccurate, especially when using presence-only data (Pearse et al. 2017), so we generated estimates of the 5th and 95th percentiles to provide more robust estimates of the onset and offset of flowering. These phenometrics were calculated using a Weibull-parameterized estimator that has been found to be fairly accurate and, importantly, unbiased in estimating these phenometrics for univoltine phenological phases (Belitz et al. 2020). We expect some estimates to be lower or higher than the "true" onset or offset values, but we do not expect these errors to be consistently an overestimation or underestimation of the "true" value, allowing for robust parameter estimates in our models.

We note that while using spatial gradients for predicting temporal changes is common practice (e.g., species distribution models), space-for-time substitutions are subject to concern (Damgaard 2019). Recognizing this issue, we have explicitly focused on relatively short-term predictions (in 10 years and 30 years). Such a short-term prediction timeline limits concerns about temporal niche conservatism. One potential way to validate our predictions is to backcast temporal trends of flowering onset, offset, and durations in different regions using phenological information derived from herbarium specimens or other historical sources. The challenges, however, are not trivial. First, it is often more difficult and labor intensive to annotate flowers from herbarium specimens, although recent advances in machine learning and annotation methods can be helpful with this task (Brenskelle et al. 2020, Pearson et al. 2020). Second, the data density of specimen-derived phenological information likely will be too low for sufficient sampling at the spatial scale used here, since records must be dense enough both spatially and temporally to estimate phenology. Nevertheless, such an approach is critical for both validating models with backcasting and understanding spatiotemporal trends. We encourage the further complete digitization of such data.

This work showcases the power of new data sources generated by citizen science and methods to understand phenology at increasingly finer spatial grain and broad, range-wide extents. The single most significant bottleneck in this effort was annotating flowering state, but even here continued automation of such tasks is within reach (Pearson et al. 2020), including potential for more detailed phenology reporting e.g., number of flowers or fruits. If annotation automation can scale with growth of research-grade citizen science photographs, phenologists will have at their fingertips a global resource capable of addressing fundamental spatial ecological questions about phenology and its change.

Data Availability. We archived a version of the image data used in this study at GBIF (https://doi.org/10.15468/dl.7cxycm). All image scores, estimated flowering onset and offset dates, contemporary and future climatic and human population density data are available on Github (https://github.com/daijiang/flower_duration) and are archived permanently at Zenodo (https://doi.org/10.5281/zenodo.3993848). Summary of number of images scored and functional traits of species are available in the Supporting Data.

Code Availability. Code used are available on Github (https://github.com/daijiang/flower_duration) and are archived permanently at Zenodo (https://doi.org/10.5281/zenodo.3993848).

Acknowledgements. We thank the many iNaturalist users who are photographing and identifying plants and whose efforts are really the engine enabling this work. We appreciate the help from Carrie Seltzer regarding how to best provide annotations back to iNaturalist. We thank Jacob McKee for access to the LandCast 2030 and LandCast 2050 datasets used here, which are used with permission. We finally note and appreciate help annotating records from Reid Rumelt and Minji Ku. No direct funding supported this effort, but R.P.G and M.W.B developed tools used in this study as part of Macrosystems proposal focused on tri-trophic phenological mismatch (NSF DEB #1703048).

Competing interests. The authors declare no competing interests.

Figures

Figure 1: **Schematic figures of different scenarios of plant flowering onset, offset, and duration (upper panel) and locations of flowering observations used (lower panel).** Each filled 25 km by 25 km cell in the lower panel represents a location where phenometrics for at least one species could be estimated. The upper panel shows three hypothetical scenarios for spatial patterns of duration include: (**a**): longer flower durations in warm areas, which can happen if flower offset is less sensitive to temperature than flower onset (slope of offset shallower than onset); (**b**): fixed flower duration across areas with different annual average temperature, where the age of the structure after onset determines senescence timing, as might occur if there is stronger genetic control rather than environmental cues for offset; (**c**): shorter durations in warm areas, which can happen if the metabolic rate of flower offset is higher than that of flower onset with higher temperature (slope of offset steeper than onset).

Figure 2: **Model predictions of flowering onset (day of year).** (**a**): Flowering onset was earlier in areas with higher annual average temperature, but the response of spring-blooming species was significantly more sensitive than that of summer-blooming species. Flowering onset was later in areas with higher temperature seasonality (**b**) and a higher number of chilling days (**c**). Shading areas indicate 95% confidence intervals hereafter.

Figure 3: **Model predictions of flowering offset (day of year).** (**a**): Flowering offset was earlier in warm areas for spring-blooming species, but was later for summer-blooming species. The flowering offset of species with different growth forms responded differently to changes in human population density (**b**, as a proxy of urbanization) and annual total precipitation (**c**). Woody plants showed higher sensitivity to both compared to herbaceous ones.

Figure 4: **Model predictions of flowering duration (number of days).** Flowering duration of summer and spring flowering species varied depending on growth forms (**a**) but was generally longer than those of spring-blooming species (**e**). (**b**) shows that flowering duration of summer-blooming species, but not spring-blooming ones, was longer in areas with higher human population density. In (**c**), flowering duration in general was shorter in areas with higher temperature seasonality, especially for woody perennial species, though they also have the longest flowering durations compared with other growth forms (**f**). Flowering durations across all species were longer in areas with more precipitation (**d**) and less chilling days in winter (**g**). Error bars represent 95% confidence intervals.

Figure 5: **Model predictions of flowering onset, offset, and duration under RCP 8.5 at 2030 and 2050.** Labels on the y-axis indicate species names and whether they are spring- or summer-blooming species. Points filled with colors represent significant deviation from 0 (black vertical lines). Blue dots show mean shifts based on RCP 8.5 at 2030 and orange dots at 2050. Error bars represent 95% confidence intervals. All results are ordered by shifts in duration at 2050. Almost all species have longer predicted mean durations and this is strongest for summer flowering plants compared to spring bloomers.

Table 1: **Summary of linear mixed models and phylogenetic linear mixed models for plant flowering onset, offset, and duration.** Summary of all fixed effects in models of onset, offset and duration fixed. Onset models primarily feature climatic drivers while offset and duration are also strongly driven by urbanization and interactions between traits and climate. Supplemental tables for each model provide details of random terms. Marginal and conditional R^2 values for each model also provided. The ":" symbol in the term column represents interaction between variables. Abbreviations: bio1, annual average temperature; bio4, temperature seasonality; bio12, annual precipitation; number of winter chilling days, number of chilling days from November 15 to the end of February; group summer_bloomer, species that are summer bloomers; pop, log-transformed human population density at 25 by 25 km resolution; growth form Herb_perennial, growth form of herb (perennial); growth form Woody_perennial, growth form of woody species (perennial). LMM: linear mixed models; *: $p < 0.05$; · : $p < 0.1$.

term	Onset_LMM	Offset_LMM	Duration_LMM
Intercept	86.97 ± 3.7 *	146.038 ± 11.9 *	60.36 ± 7.6 *
bio1	-16.204 ± 1.6 *	-16.701 ± 1.5 *	9.264 ± 3 *
bio4	7.813 ± 1.7 *		-6.146 ± 3.2 ·
number of winter chilling days	3.276 ± 1 *		-6.054 ± 1.2 *
group summer_bloomer	93.914 ± 6.8 *	127.938 ± 12.4 *	40.005 ± 7.9 *
bio12		-0.852 ± 1.3	1.623 ± 1.1
pop		3.212 ± 1.3 *	-0.276 ± 1.1
growth form Herb_perennial		-10.334 ± 12.9	-14.004 ± 8.2 ·
growth form Woody_perennial		24.882 ± 19.7	22.6 ± 12.9 ·
bio1:group summer_bloomer	10.201 ± 2.7 *	25.431 ± 2.4 *	10.455 ± 2.7 *
pop:growth form Herb_perennial		-1.116 ± 1.4	
pop:growth form Woody_perennial		9.024 ± 2.3 *	
bio12:growth form Herb_perennial		3.34 ± 1.5 *	

bio12:growth form Woody_perennial		6.993 ± 2.8 *	
pop:group summer_boolmer			4.405 ± 2 *
bio1:growth form Herb_perennial			-8.971 ± 3.1 *
bio1:growth form Woody_perennial			-13.106 ± 4.8 *
bio4:growth form Herb_perennial			-6.954 ± 3.8 ·
bio4:growth form Woody_perennial			-31.714 ± 5.8 *
Marginal R^2	0.746	0.634	0.425
Conditional R^2	0.919	0.928	0.691

References

Barve, V. V., L. Brenskelle, D. Li, B. J. Stucky, N. V. Barve, M. M. Hantak, B. S. McLean, D. J. Paluh, J. A. Oswald, M. W. Belitz, and others. 2020. Methods for broad-scale plant phenology assessments using citizen scientists' photographs. Applications in plant sciences 8.

Bates, D., M. Mächler, B. Bolker, and S. Walker. 2015. Fitting linear mixed-effects models using lme4. Journal of Statistical Software 67:1–48.

Belitz, M. W., E. A. Larsen, L. Ries, and R. P. Guralnick. 2020. The accuracy of phenology estimators for use with sparsely sampled presence-only observations. Methods in Ecology and Evolution.

Brenskelle, L., R. P. Guralnick, M. Denslow, and B. J. Stucky. 2020. Maximizing human effort for analyzing scientific images: A case study using digitized herbarium sheets. Applications in Plant Sciences 8:e11370.

CaraDonna, P. J., A. M. Iler, and D. W. Inouye. 2014. Shifts in flowering phenology reshape a subalpine plant community. Proceedings of the National Academy of Sciences 111:4916–4921.

Cleland, E. E., I. Chuine, A. Menzel, H. A. Mooney, and M. D. Schwartz. 2007. Shifting plant phenology in response to global change. Trends in ecology & evolution 22:357–365.

Crimmins, T. M., M. A. Crimmins, and C. D. Bertelsen. 2013. Spring and summer patterns in flowering onset, duration, and constancy across a water-limited gradient. American journal of botany 100:1137–1147.

Damgaard, C. 2019. A critique of the space-for-time substitution practice in community ecology. Trends in ecology & evolution 34:416–421.

Fang, Y., and J. W. Jawitz. 2018. High-resolution reconstruction of the united states human population distribution, 1790 to 2010. Scientific data 5.

Felsenstein, J. 1985. Phylogenies and the comparative method. The American Naturalist 125:1–15.

Garamszegi, L. Z. 2014. Modern phylogenetic comparative methods and their application in evolutionary biology: Concepts and practice. Springer.

Grimm, N. B., S. H. Faeth, N. E. Golubiewski, C. L. Redman, J. Wu, X. Bai, and J. M. Briggs. 2008. Global change and the ecology of cities. science 319:756–760.

Hinchliff, C. E., S. A. Smith, J. F. Allman, J. G. Burleigh, R. Chaudhary, L. M. Coghill, K. A. Crandall, J. Deng, B. T. Drew, R. Gazis, and others. 2015. Synthesis of phylogeny and taxonomy into a comprehensive tree of life. Proceedings of the National Academy of Sciences 112:12764–12769.

Hopkins, A. D. 1920. The bioclimatic law. Journal of the Washington Academy of Sciences 10:34–40.

Høye, T. T., E. Post, N. M. Schmidt, K. Trøjelsgaard, and M. C. Forchhammer. 2013. Shorter flowering seasons and declining abundance of flower visitors in a warmer arctic. Nature climate change 3:759–763.

Jochner, S., and A. Menzel. 2015. Urban phenological studies–past, present, future. Environmental pollution 203:250–261.

Kerby, J. T., and E. Post. 2013. Advancing plant phenology and reduced herbivore production in a terrestrial system associated with sea ice decline. Nature Communications 4:1–6.

Kudo, G., and E. J. Cooper. 2019. When spring ephemerals fail to meet pollinators: Mechanism of phenological mismatch and its impact on plant reproduction. Proceedings of the Royal Society B 286:20190573.

Kudo, G., and T. Y. Ida. 2013. Early onset of spring increases the phenological mismatch between plants and pollinators. Ecology 94:2311–2320.

Kuznetsova, A., P. B. Brockhoff, and R. H. B. Christensen. 2017. lmerTest package: Tests in linear mixed effects models. Journal of Statistical Software 82:1–26.

Larcher, W. 2003. Physiological plant ecology: Ecophysiology and stress physiology of functional groups. Springer Science & Business Media.

Lessard-Therrien, M., T. J. Davies, and K. Bolmgren. 2014. A phylogenetic comparative study of flowering phenology along an elevational gradient in the canadian subarctic. International Journal of Biometeorology 58:455–462.

Li, D., R. Dinnage, L. A. Nell, M. R. Helmus, and A. R. Ives. 2020. Phyr: An r package for phylogenetic species-distribution modelling in ecological communities. Methods in Ecology and Evolution 11:1455–1463.

Li, D., and A. R. Ives. 2017. The statistical need to include phylogeny in trait-based analyses of community composition. Methods in Ecology and Evolution 8:1192–1199.

Li, D., B. J. Stucky, J. Deck, B. Baiser, and R. P. Guralnick. 2019. The effect of urbanization on plant phenology depends on regional temperature. Nature ecology & evolution 3:1661–1667.

Linderholm, H. W. 2006. Growing season changes in the last century. Agricultural and forest meteorology 137:1–14.

Marchin, R. M., C. F. Salk, W. A. Hoffmann, and R. R. Dunn. 2015. Temperature alone does not explain phenological variation of diverse temperate plants under experimental warming. Global Change Biology 21:3138–3151.

McKee, J. J., A. N. Rose, E. A. Bright, T. Huynh, and B. L. Bhaduri. 2015. Locally adaptive, spatially explicit projection of us population for 2030 and 2050. Proceedings of the National Academy of Sciences 112:1344–1349.

Meinshausen, M., S. J. Smith, K. Calvin, J. S. Daniel, M. Kainuma, J.-F. Lamarque, K. Matsumoto, S. Montzka, S. Raper, K. Riahi, and others. 2011. The rcp greenhouse gas concentrations and their extensions from 1765 to 2300. Climatic change 109:213.

Menzel, A., and P. Fabian. 1999. Growing season extended in europe. Nature 397:659–659.

Mouradov, A., F. Cremer, and G. Coupland. 2002. Control of flowering time: Interacting pathways as a basis for diversity. The Plant Cell 14:S111–S130.

Murray, M., M. Cannell, and R. Smith. 1989. Date of budburst of fifteen tree species in britain following climatic warming. Journal of Applied Ecology:693–700.

Parmesan, C. 2007. Influences of species, latitudes and methodologies on estimates of phenological response to global warming. Global Change Biology 13:1860–1872.

Pearse, W. D., Davis, C. C., Inouye, D. W., Primack, R. B., & Davies, T. J. 2017. A statistical estimator for determining the limits of contemporary and historic phenology. Nature Ecology & Evolution, 1: 1876-1882.

Pearson, K. D., G. Nelson, M. F. Aronson, P. Bonnet, L. Brenskelle, C. C. Davis, E. G. Denny, E. R. Ellwood, H. Goëau, J. M. Heberling, and others. 2020. Machine learning using digitized herbarium specimens to advance phenological research. BioScience 70:610–620.

Petanidou, T., A. S. Kallimanis, S. P. Sgardelis, A. D. Mazaris, J. D. Pantis, and N. M. Waser. 2014. Variable flowering phenology and pollinator use in a community suggest future phenological mismatch. Acta Oecologica 59:104–111.

Peters, G. P., R. M. Andrew, T. Boden, J. G. Canadell, P. Ciais, C. Le Quéré, G. Marland, M. R. Raupach, and C. Wilson. 2012. The challenge to keep global warming below 2 c. Nature Climate Change 3:4.

PRISM Climate Group. 2004. PRISM climate data. Oregon State University, http://prism.oregonstate.edu, created 4 Feb 2004.

Rafferty, N. E., C. D. Bertelsen, and J. L. Bronstein. 2016. Later flowering is associated with a compressed flowering season and reduced reproductive output in an early season floral resource. Oikos 125:821–828.

Renner, S. S., and C. M. Zohner. 2018. Climate change and phenological mismatch in trophic interactions among plants, insects, and vertebrates. Annual Review of Ecology, Evolution, and Systematics 49:165–182.

Richardson, A. D., and J. O'Keefe. 2009. Phenological differences between understory and overstory. Pages 87–117 *in* Phenology of ecosystem processes. Springer.

Schenk, M., J. Krauss, and A. Holzschuh. 2018. Desynchronizations in bee–plant interactions cause severe fitness losses in solitary bees. Journal of Animal Ecology 87:139–149.

Semenchuk, P. R., M. A. Gillespie, S. B. Rumpf, N. Baggesen, B. Elberling, and E. J. Cooper. 2016. High arctic plant phenology is determined by snowmelt patterns but duration of phenological periods is fixed: An example of periodicity. Environmental Research Letters 11:125006.

Sherry, R. A., X. Zhou, S. Gu, J. A. Arnone, D. S. Schimel, P. S. Verburg, L. L. Wallace, and Y. Luo. 2007. Divergence of reproductive phenology under climate warming. Proceedings of the National Academy of Sciences 104:198–202.

Smith, S. A., and J. W. Brown. 2018. Constructing a broadly inclusive seed plant phylogeny. American journal of botany 105:302–314.

Stinson, K. A., J. M. Albertine, L. M. Hancock, T. G. Seidler, and C. A. Rogers. 2016. Northern ragweed ecotypes flower earlier and longer in response to elevated co 2: What are you sneezing at? Oecologia 182:587–594.

Taylor, K. E., R. J. Stouffer, and G. A. Meehl. 2012. An overview of cmip5 and the experiment design. Bulletin of the American Meteorological Society 93:485–498.

Theobald, E. J., I. Breckheimer, and J. HilleRisLambers. 2017. Climate drives phenological reassembly of a mountain wildflower meadow community. Ecology 98:2799–2812.

Thrasher, B., E. P. Maurer, P. B. Duffy, and C. McKellar. 2012. Bias correcting climate model simulated daily temperature extremes with quantile mapping.

Thrasher, B., J. Xiong, W. Wang, F. Melton, A. Michaelis, and R. Nemani. 2013. Downscaled climate projections suitable for resource management. Eos, Transactions American Geophysical Union 94:321–323.

Tylianakis, J. M., R. K. Didham, J. Bascompte, and D. A. Wardle. 2008. Global change and species interactions in terrestrial ecosystems. Ecology letters 11:1351–1363.

Visser, M. E., and C. Both. 2005. Shifts in phenology due to global climate change: The need for a yardstick. Proceedings of the Royal Society B: Biological Sciences 272:2561–2569.

Visser, M. E., and P. Gienapp. 2019. Evolutionary and demographic consequences of phenological mismatches. Nature ecology & evolution 3:879–885.

Wang, Y., X.-D. Yang, A. Ali, G.-H. Lv, Y.-X. Long, Y.-Y. Wang, Y.-G. Ma, and C.-C. Xu. 2020. Flowering phenology shifts in response to functional traits, growth form, and phylogeny of woody species in a desert area. Frontiers in Plant Science 11:536.

Wohlfahrt, G., E. Tomelleri, and A. Hammerle. 2019. The urban imprint on plant phenology. Nature Ecology & Evolution 3:1668–1674.

Wolkovich, E. M., and E. E. Cleland. 2011. The phenology of plant invasions: A community ecology perspective. Frontiers in Ecology and the Environment 9:287–294.

Yang, J., and E. Bou-Zeid. 2018. Should cities embrace their heat islands as shields from extreme cold? Journal of Applied Meteorology and Climatology 57:1309–1320.

Zohner, C. M., L. Mo, and S. S. Renner. 2018. Global warming reduces leaf-out and flowering synchrony among individuals. Elife 7:e40214.

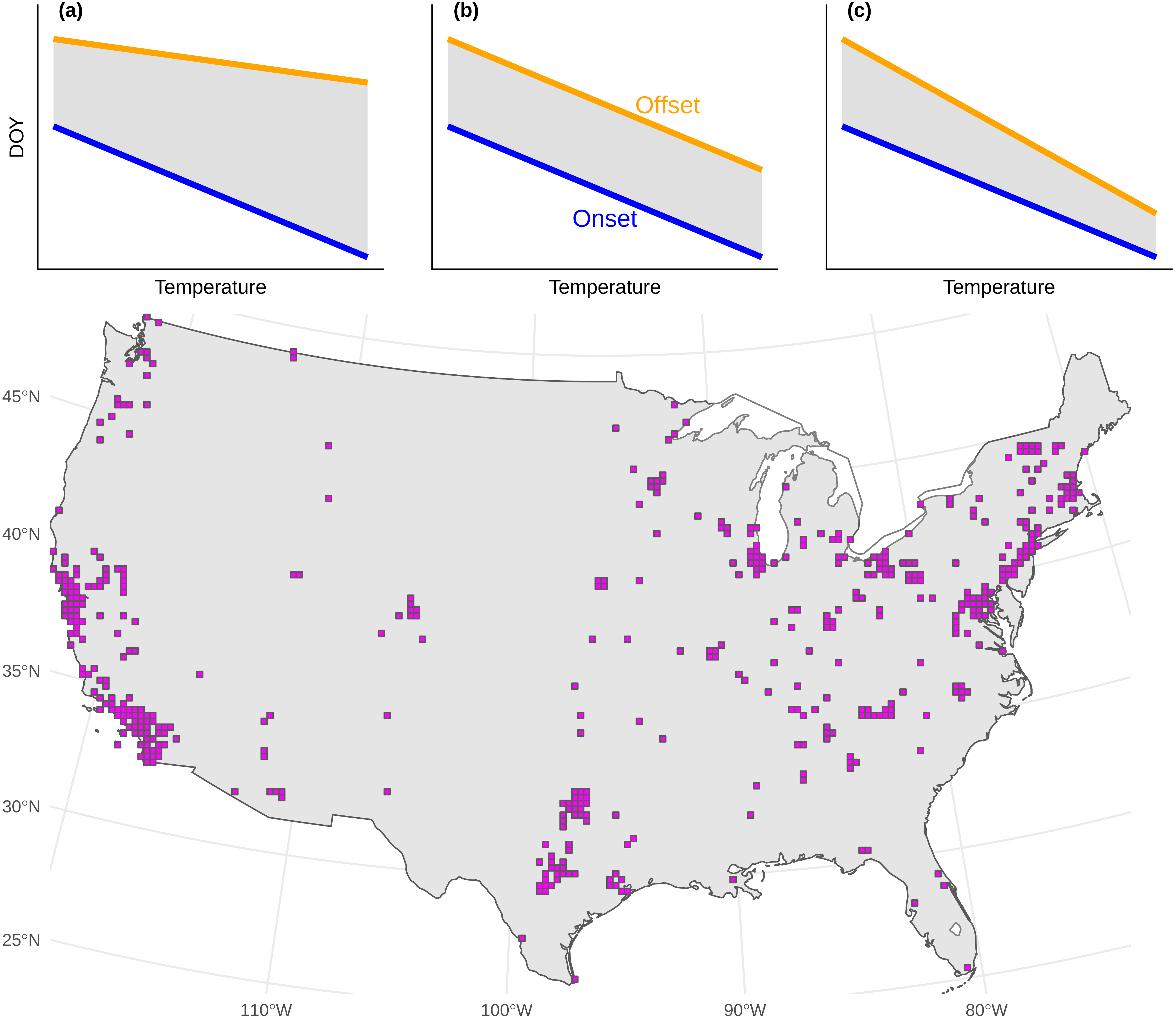
(a)
(b)
(c)
DOY
Offset
Onset
Temperature
Temperature
Temperature
45°N
40°N
35°N
30°N
25°N
110°W
100°W
90°W
80°W

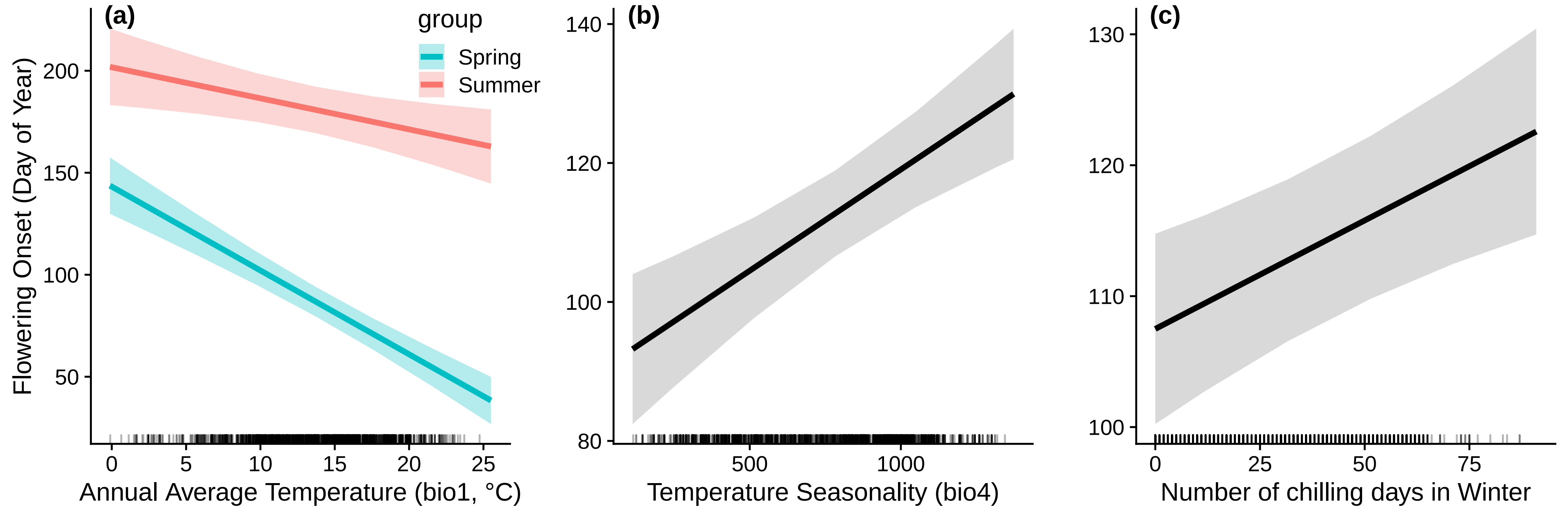
(a)
group
Spring
Summer
Flowering Onset (Day of Year)
200
150
100
50
0
5
10
15
20
25
Annual Average Temperature (bio1, °C)
(b)
140
120
100
80
500
1000
Temperature Seasonality (bio4)
(c)
130
120
110
100
0
25
50
75
Number of chilling days in Winter

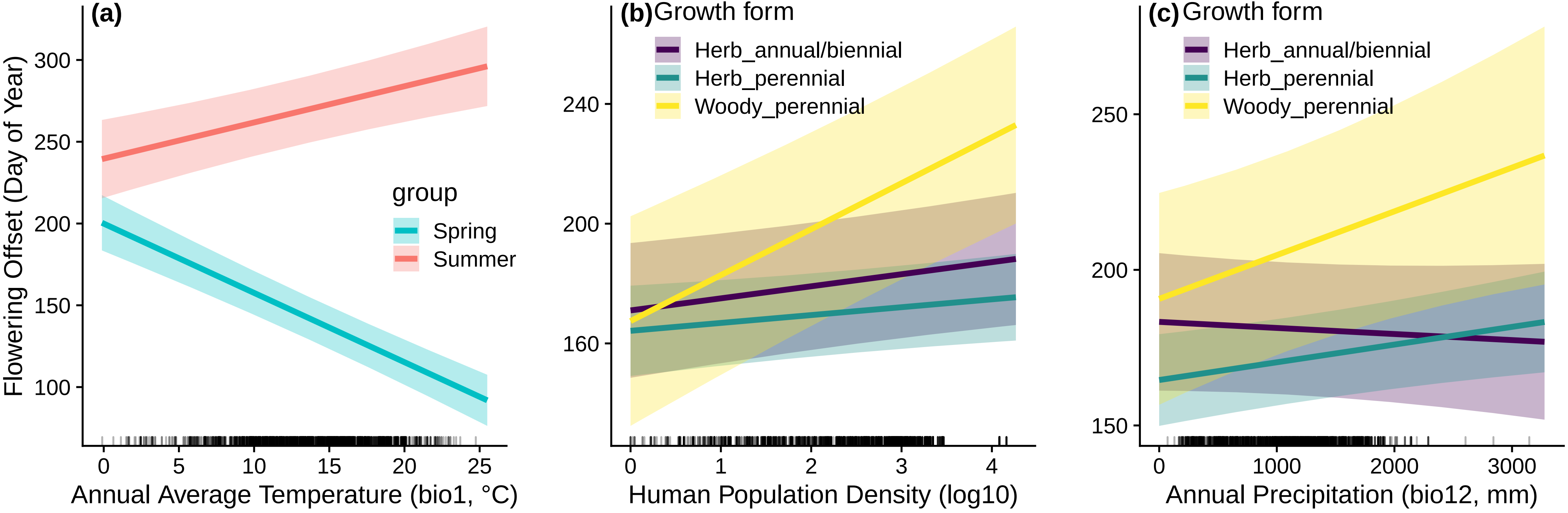
(a)
Flowering Offset (Day of Year)
300
250
200
150
100
group
Spring
Summer
0
5
10
15
20
25
Annual Average Temperature (bio1, °C)
(b)
Growth form
Herb_annual/biennial
Herb_perennial
Woody_perennial
240
200
160
0
1
2
3
4
Human Population Density (log10)
(c)
Growth form
Herb_annual/biennial
Herb_perennial
Woody_perennial
250
200
150
0
1000
2000
3000
Annual Precipitation (bio12, mm)

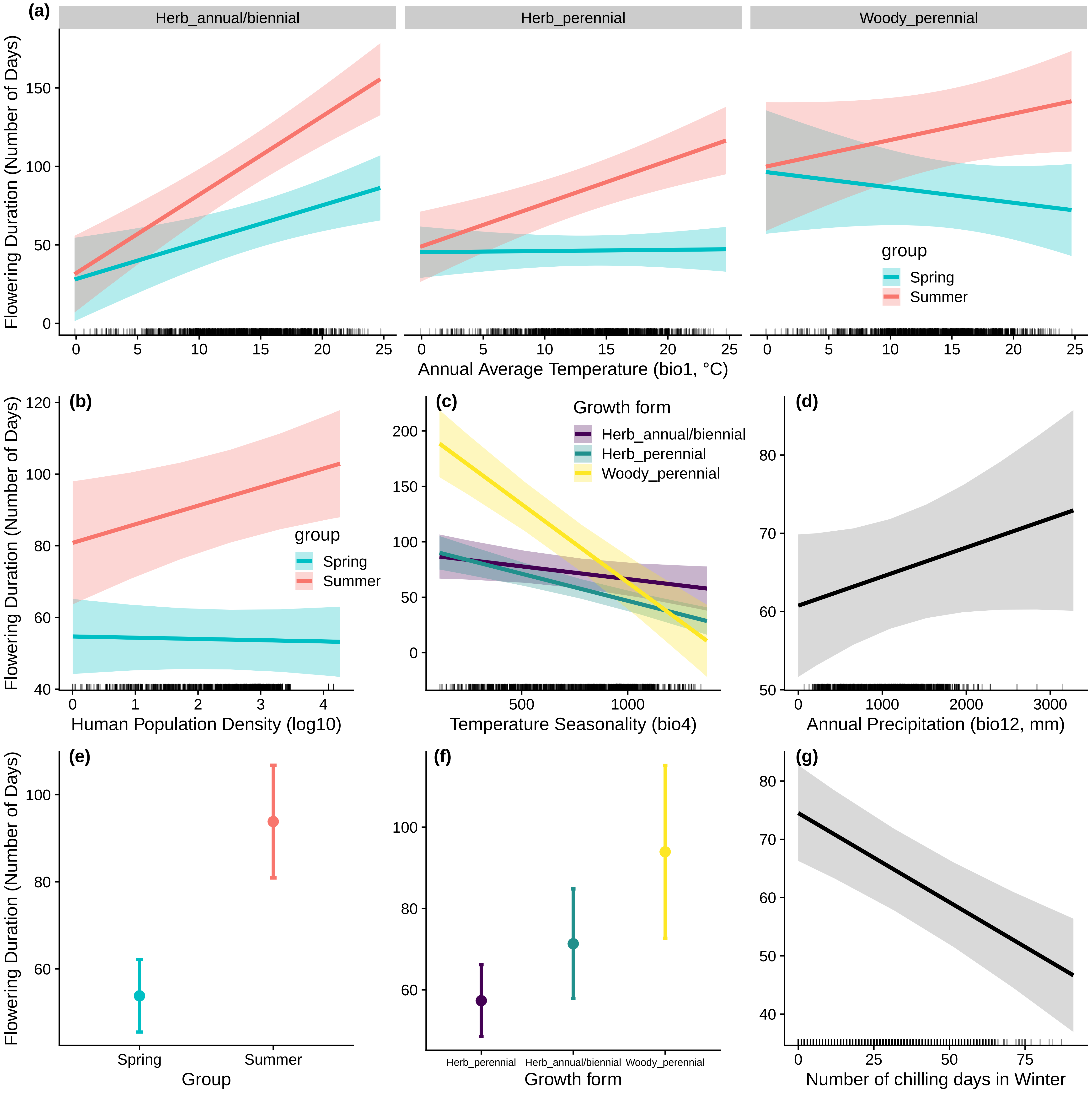
(a)
Herb_annual/biennial
Herb_perennial
Woody_perennial
Flowering Duration (Number of Days)
0
50
100
150
0
5
10
15
20
25
Annual Average Temperature (bio1, °C)
group
Spring
Summer
(b)
Flowering Duration (Number of Days)
40
60
80
100
120
0
1
2
3
4
Human Population Density (log10)
group
Spring
Summer
(c)
Growth form
Herb_annual/biennial
Herb_perennial
Woody_perennial
0
50
100
150
200
500
1000
Temperature Seasonality (bio4)
(d)
50
60
70
80
0
1000
2000
3000
Annual Precipitation (bio12, mm)
(e)
Flowering Duration (Number of Days)
60
80
100
Spring
Summer
Group
(f)
60
80
100
Herb_perennial
Herb_annual/biennial
Woody_perennial
Growth form
(g)
40
50
60
70
80
0
25
50
75
Number of chilling days in Winter

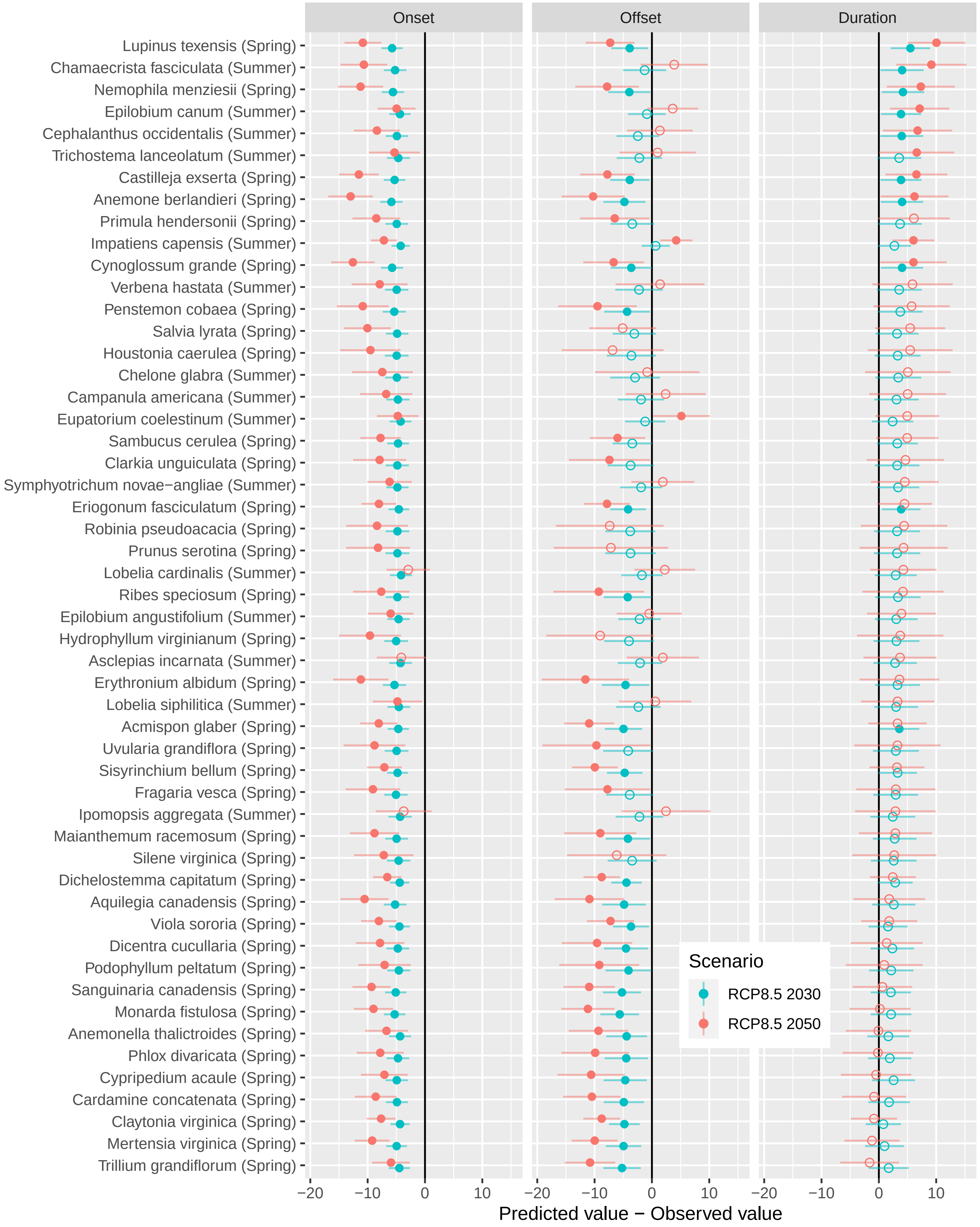
Onset
Offset
Duration
Lupinus texensis (Spring)
Chamaecrista fasciculata (Summer)
Nemophila menziesii (Spring)
Epilobium canum (Summer)
Cephalanthus occidentalis (Summer)
Trichostema lanceolatum (Summer)
Castilleja exserta (Spring)
Anemone berlandieri (Spring)
Primula hendersonii (Spring)
Impatiens capensis (Summer)
Cynoglossum grande (Spring)
Verbena hastata (Summer)
Penstemon cobaea (Spring)
Salvia lyrata (Spring)
Houstonia caerulea (Spring)
Chelone glabra (Summer)
Campanula americana (Summer)
Eupatorium coelestinum (Summer)
Sambucus cerulea (Spring)
Clarkia unguiculata (Spring)
Symphyotrichum novae−angliae (Summer)
Eriogonum fasciculatum (Spring)
Robinia pseudoacacia (Spring)
Prunus serotina (Spring)
Lobelia cardinalis (Summer)
Ribes speciosum (Spring)
Epilobium angustifolium (Summer)
Hydrophyllum virginianum (Spring)
Asclepias incarnata (Summer)
Erythronium albidum (Spring)
Lobelia siphilitica (Summer)
Acmispon glaber (Spring)
Uvularia grandiflora (Spring)
Sisyrinchium bellum (Spring)
Fragaria vesca (Spring)
Ipomopsis aggregata (Summer)
Maianthemum racemosum (Spring)
Silene virginica (Spring)
Dichelostemma capitatum (Spring)
Aquilegia canadensis (Spring)
Viola sororia (Spring)
Dicentra cucullaria (Spring)
Podophyllum peltatum (Spring)
Sanguinaria canadensis (Spring)
Monarda fistulosa (Spring)
Anemonella thalictroides (Spring)
Phlox divaricata (Spring)
Cypripedium acaule (Spring)
Cardamine concatenata (Spring)
Claytonia virginica (Spring)
Mertensia virginica (Spring)
Trillium grandiflorum (Spring)
−20
−10
0
10
−20
−10
0
10
−20
−10
0
10
Predicted value − Observed value
Scenario
RCP8.5 2030
RCP8.5 2050